Biomacromolecules

pubs.acs.org/Biomac
Article

Autonomous Abiotic Thermal Protectant for Immunoglobulin G: Reducing the Need for Cold Chain Storage

Beverly Chou, Rishad J. Dalal, and Kenneth J. Shea*

Cite This: Biomacromolecules 2025, 26, 2825−2834

Read Online

ACCESS | Metrics & More | Article Recommendations | Supporting Information

ABSTRACT: Antibodies are vital biologic therapeutics, but their impact is limited by thermal instability. This requires maintaining a cold chain, from the point of manufacture to the point of use. We report an approach that could reduce the need for a cold chain. We present a thermal protectant (TP) for immunoglobulin G (IgG) that mimics the behavior of the heat shock protein HSP60. This hydrogel copolymer nanoparticle shows minimal affinity for IgG at or below 25 °C. As temperatures rise and approach the proteins melting temperature (T_m), the TP undergoes an autonomous phase transition (~27 °C), above which the TP shows high affinity for IgG sequestering and stabilizing IgG at temperatures far above T_m. As temperatures return to RT, the TP reverts to its water-swollen state, allowing any metastable proteins time to refold to their native state before being released. The optimized TP has very low IgG molar capacity, effectively isolating and preventing aggregation at elevated temperatures.

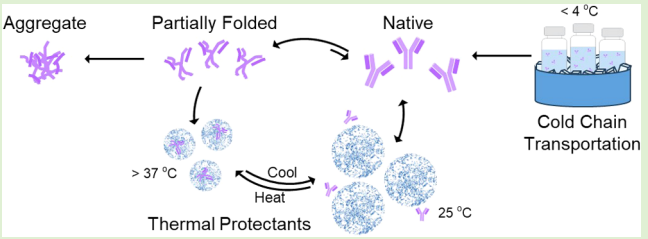

INTRODUCTION

Biological therapeutics, including antibodies, vaccines, recombinant hormones/proteins, and cellular and gene-based biologics, now play a prominent role in contemporary medicine.[1] Proteins, particularly monoclonal antibodies, represent a significant portion of the market[2−4] and contribute significantly to global health. Despite their importance, there are well-known limitations to protein, peptide, and other biological therapeutics that restrict their impact.[4]

A key area is their vulnerability to extreme temperatures, which imposes constraints on their distribution, storage, and availability. Most proteins and peptides require temperature management; following their production, they typically require a cold chain for their delivery and storage.[5] The cold chain, a system of storing and transporting temperature-sensitive products from the point of manufacture to the point of use, requires meticulous management to maintain the safety and potency of pharmaceuticals and vaccines during storage, transport, and service delivery.[6] Maintaining the cold chain necessitates extensive infrastructure that is expensive to build and maintain. This poses a significant challenge for equitable healthcare delivery by limiting availability to locations that can reliably supply a cold chain infrastructure. A recent perspective identified a grand challenge in pharmaceutical research: innovations are needed in the design, formulation, and biomanufacturing of biologics.[7] Although progress is being made on many fronts, including incorporating lessons from thermophilic organisms,[8] there is no general practical solution to this problem. As a result, widespread availability of many biomacromolecule therapeutics remains limited. The problem is particularly acute when rare, valuable therapeutics, such as IgG-based snake antivenoms, are needed in locations that are least served by a reliable cold chain.[9,10]

In nature, heat shock proteins (HSPs) are biologics found in both prokaryotic and eukaryotic organisms. They play a crucial role in maintaining cellular proteostasis and protecting cells from stress. Acting as molecular chaperones, HSPs assist in the folding of newly synthesized polypeptides, refold metastable proteins, and perform many other functions. HSPs are recruited to process damaged or misfolded proteins,[11−13] which expose hydrophobic domains, rendering them susceptible to aggregation and misfolding. For example, HSP60 functions by binding and isolating a metastable protein in a hydrophobic chamber.[11−13] Once bound, a second protein closes off the hydrophobic chamber isolating the metastable protein. An ATP-driven event then induces a conformational change that transforms the hydrophobic chamber into a more hydrophilic microenvironment, allowing the isolated metastable protein time to refold to its native state. HSPs have served as inspiration for scientists to create materials and artificial variants to stabilize and protect proteins. However, it should be noted that field applications of therapeutic proteins are often exposed to conditions harsher than those in living organisms. For example, temperatures at delivery locations can

Received: October 28, 2024
Revised: March 28, 2025
Accepted: March 31, 2025
Published: April 7, 2025

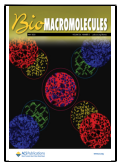

often exceed 43 °C (110 °F), requiring thermal protectants (TPs) that provide greater protection than biological HSPs.

There is a substantial body of literature that addresses protein stabilization and thermal protection, with many efforts mimicking biological HSPs. Some of the better-known strategies employ carbohydrate additives such as trehalose and related sugars, materials known for many years to stabilize proteins.[14,15] Carbohydrates are also used to enhance protein recovery following lyophilization.[16] In addition to biological carbohydrate additives, there has been a significant effort to develop synthetic polymers to stabilize proteins. This topic was the focus of a recent extensive review by Sivasankaran and coworkers.[17] Over the past 15 years, numerous innovative attempts have been made to replicate the performance of HSPs using synthetic polymer materials, beginning with the early work of Rotello,[18] Akiyoshi,[19] Shi,[20] and others. Several reviews of this research have recently been published.[21,22]

Drawing from this background one can envision an ideal TP with little to no affinity for the protein at room temperature but would autonomously protect a therapeutic protein such as immunoglobulin G (IgG) from denaturation and aggregation at elevated temperatures. As temperatures rise and approach and exceed the melting temperature of the protein (T_m), hydrophobic domains of the protein are often exposed, rendering them susceptible to denaturation and aggregation. To sequester the vulnerable protein, the TP should transform to an entity that binds IgG at elevated temperatures, isolating it from solution and limiting opportunities for denaturation and aggregation. As temperatures fall, the TP should undergo an autonomous change of microenvironment, triggering the release of the metastable protein into a hydrophilic environment conducive to refolding. The time scale for this is critical, but fortunately the kinetics of partially denatured protein refolding are extremely fast.[23] As temperatures continue to fall, renatured protein is released from the TP and should be easily removed from the TP and aggregated IgG at normal temperatures by filtration-centrifugation. We have previously reported methods for producing *N*-isopropylacrylamide (NIPAm)-based synthetic hydrogel copolymers engineered with affinity and specificity for target proteins and peptides.[24] NIPAm-based hydrogel copolymer nanoparticles (NPs) are often temperature sensitive, providing an opportunity for autonomous protein capture and release.[25−28] In earlier work, synthetic hydrogel copolymers were engineered with affinity and specificity for IgG using aliphatic hydrophobic groups, although their thermal responsiveness was not useful for the current application.[29,30] Nevertheless, this work guided our initial selection of functional monomers to screen hydrogel copolymers with properties for a TP. In this manuscript, we describe a TP, a hydrogel NP, that meets these criteria. When added to a therapeutically important protein class (IgG), as temperatures rise above RT, the TP undergoes an autonomous transition to an entity that binds IgG. At temperatures at or above T_m, the TP was optimized to capture and isolate IgG molecules, minimizing irreversible denaturation and aggregation. Upon cooling to RT, the TP undergoes a conformational change from hydrophobic to hydrophilic, decreasing its interaction with IgG, allowing the liberated IgG time to refold to its native state before being released from the TP. These properties mimic those of HSP60 and offer a potential TP that could reduce the need for a cold chain.

MATERIALS AND METHODS

Materials. The following materials were obtained from commercial sources: NIPAm and acrylic acid (AAc) were obtained from Aldrich; polyclonal IgG from human serum with and without FITC label was obtained from Jackson ImmunoResearch; and *N*,*N*′-methylenebis(acrylamide) (BIS) was from Fluka. All other solvents and compounds were obtained from Fisher Scientific Inc. or VWR International LLC. NIPAm was crystallized from hexane before use. AAc was purified using vacuum distillation over copper wire. *N*-hexylacrylamide (HAm) and *N*-octylacrylamide (OAm) were synthesized from previously published procedures.[31] Other chemicals were used as received. Water used in polymerization and characterization was purified using a Barnstead Nanopure Diamond system. Labconco Freezone 2.5 was used for lyophilization.

NP Synthesis. NPs were synthesized using a modified free radical precipitation polymerization.[32−38] Briefly, stock solutions of NiPAm (A mol %), AAc (B mol %), BIS (2 mol %), and SDS (0.04−0.16 mg/mL) were prepared by dissolving the monomers in nanopure water. The OAm, HAm, and tBAm (C mol %) stock solutions were prepared by dissolving the monomers in a minimal amount of ethanol (Figure 1). Monomers were added in the desired ratios to generate a total

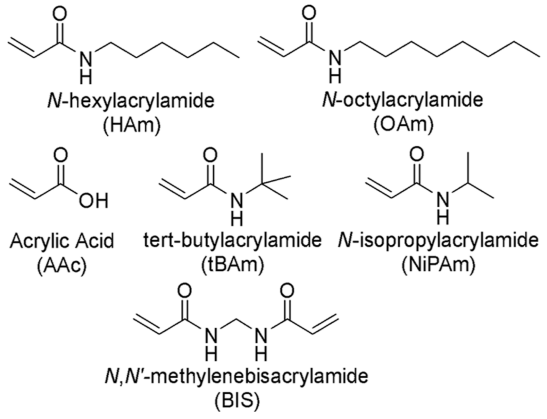

Figure 1. Monomers used in this study.

monomer concentration of 65 mM in 25 mL of water. The solutions were degassed for 30 min with nitrogen while stirring. The initiator (APS, 0.6 mg/mL) was dissolved in a minimal volume of acetone (~200 μL). The initiator was then injected into the reaction mixture after degassing, and the flask was immersed into an oil bath at 60 °C for 3 h with stirring under a nitrogen atmosphere. The polymer solutions were purified by dialysis against deionized water (4 L for 100 mL crude NP) using a 12−14 kDa MWCO regenerated cellulose membrane and changing the water twice daily for 2 d. After dialysis, 5 mL of the NP solution was lyophilized to determine weight-based concentration and yield.

NP Characterization. Dynamic Light Scattering (DLS). The DLS measurements were performed using the Zeta-sizer Nano DLS (Malvern). NP solutions were diluted 10× from dialyzed solutions and scanned for average hydrodynamic radius (R_h) at room temperature in nanopure water.

The temperature-induced volume change (ΔV, Table S1B) was calculated using Rh determined by DLS at the NPs largest and smallest sizes measured, assuming the NPs are spherical

$$\Delta V = (4/3\pi R_{h(\text{above LCST})^3}) - (4/3\pi R_{h(\text{above LCST})^3})$$

Multiangle Light Scattering and Refractive Index. The weight-averaged molecular weight (Mw), radius of gyration (Rg), and refractive index (RI) increment (dn/dc) values for the NPs were determined using batch mode injection of NP solutions with increasing concentrations that varied for each NP from 1−250 μg/mL. Molecular weight measurements were determined using the DAWN-HELEOS (Wyatt Technology Corporation) instrument

https://doi.org/10.1021/acs.biomac.4c01492
Biomacromolecules 2025, 26, 2825−2834

Table 1. Summary of NP Compositions Used and Their Yields

sample name	tBAm (mol %)	OAm (mol %)	HAm (mol %)	AAc (mol %)	NiPAm (mol %)	BIS (mol %)	yield (%)
tBAm5AAc20	5			20	73	2	84
tBAm5AAc35	5			35	58	2	68
OAm5AAc20		5		20	73	2	52
OAm5AAc35		5		35	58	2	56
HAm5AAc20			5	20	73	2	59
HAm5AAc35			5	35	58	2	42

Table 2. Summary of NP Analysis Data Obtained by DLS, MALS, and RI, Measured at 25 °C in DI Water (pH 5.5)

sample name	R_h (nm, DLS)	R_g (nm, MALS)	R_g/R_h	ρ ($\times 10^{-2}$ g/mL)	PDI (DLS)	M_W (MALS, $\times 10^6$)	dn/dc
tBAm5AAc20	414	248	0.60	0.01	0.07	18 ± 16	0.135
tBAm5AAc35	126	81	0.64	0.11	0.24	5.6 ± 2.7	0.163
OAm5AAc20	83	177	2.17	1.6	0.18	23 ± 2.9	0.149
OAm5AAc35	118	74	0.63	0.75	0.09	31 ± 1.9	0.189
HAm5AAc20	142	104	0.62	0.64	0.08	46 ± 6.9	0.170
HAm5AAc35	139	100	0.67	0.87	0.08	59 ± 4.0	0.175

attached to the Optilab rEX (Wyatt Technology Corporation) system to determine MALS and dn/dc, respectively. The data collection and analysis were performed using the Astra software (Wyatt Technology Corporation), and the data were fit using a Zimm plot.

Density measurements were determined by calculating the molecular weight of one NP, as determined by MALS, per volume of one NP, as determined by DLS

$$\rho = (\mathrm{MW}_{\mathrm{MALS}}/6.022 \times 10^{23})/(4/3\pi R_h^3)$$

Nuclear Magnetic Resonance Spectroscopy. Nuclear magnetic resonances (NMRs) were run using a Bruker AVANCE600 instrument with a BBO probe (600 MHz), and analysis was done using the XwinNMR and MestReNova programs. NP solutions were either lyophilized, then redispersed into a solution of deuterated methanol, or used in the original water solution at 5 mg/mL and contained 10% D2O for NMR field frequency locking, then run with solvent suppression to remove the water peak.

Titrations to Determine AAc Content. NP samples (12 mL) were diluted to 0.1 mg/mL in nanopure water. NaOH (0.001 M) was then slowly titrated at ∼1 drop/s into the NP solution with stirring, and the pH was measured using a Vernier pH meter. A Vernier drop counter was used to determine the volume of NaOH added during the titration, and the results were plotted using Logger Pro 3.8.7. The AAc content was determined as mols of AAc added per g NP by calculating mols of NaOH added at the end point per g NP used in the titration.

IgG Assay—Affinity. Each NP (100 μg/mL) was mixed with FITC-IgG (20 μg/mL) in sodium phosphate buffer (SPB) (35 mM, pH 5.5) to a total volume of 500 μL and heated up to 37 °C for 30 min. The NPs were then pelleted at 15 kRPM for 45 min, and the supernatant (410 μL) was removed for analysis. The pellet was reconstituted with 410 μL of PBS (35 mM, 150 mM NaCl, pH 7.3), and the mixture was incubated at RT for 30 min. The NPs were then pelleted at 14 kRPM at 16 °C for 45 min, and the supernatant was removed for analysis. Samples were analyzed at Ex 485 nm and Em 515 nm.

IgG Assay—TP. Each NP (1 mg/mL) was mixed with FITC-IgG (150 μg/mL) in SPB (35 mM, pH 5.5) to a total volume of 500 μL and heated up to 60 °C for 5 min. The NPs were then pelleted at 15 kRPM (21,130 rcf) for 45 min, and the supernatant A (410 μL) was removed. The pellet was reconstituted with 410 μL of PBS (35, 150 mM NaCl, pH 7.3), and the mixture was incubated at 4 °C for 2 h. The NPs were then pelleted at 14 kRPM (18,407 rcf) at 16 °C for 45 min, and the supernatant B was removed. The supernatant B samples were run through an HPLC size exclusion chromatography (SEC) column (TOSOH G4000SWXL) and run in SPB (100 mM, pH 7.0) at 0.75 mL/min for 25 min with UV detection at 220 nm.

The supernatant B was further analyzed by CD. The samples were analyzed from 197−250 nm at RT. Each result was averaged over 10 runs. A background scan using PBS buffer was subtracted from every sample.

IgG-NP Stoichiometry Calculation. Stoichiometry was calculated by comparing the mol of IgG captured to the mol of NP used determined by the IgG Assay−Affinity experiment. IgG molecular weight was assumed to be approximately 150 kDa, while each NP molecular weight was determined by MALS

$$\begin{aligned}&\text{mol of IgG captured/mol of NP used}\\&= (\text{IgG conc } (\mu\text{g/mL}) \times \text{IgG MW} \times \%\text{IgG captured})\\&\quad /(\text{NPconc } (\mu\text{g/mL}) \times \text{NP MW})\end{aligned}$$

VP-DSC. Samples were analyzed using a VP-DSC calorimeter (MicroCal Inc.) with a cell volume of 0.5 mL. The solutions were prepared with 200 μg/mL of IgG in SPB (35 mM, pH 5.6), with NPs (1 mg/mL). Two types of control solutions were made, either without IgG or without NPs. The SPB solution was added in its place. Each sample was degassed under vacuum (14 psi) with stirring for at least 5 min at RT immediately prior to injection. The samples were analyzed from 15−90 °C at an increase of 50 °C/h at a pressure of ∼25 psi. A solution of SPB (35 mM, pH 5.6) was used in the reference cell. Each thermogram was analyzed using Origin 7.0 software supplied the manufacturer, a blank run of buffer in buffer was first subtracted from each thermogram. The baseline was then corrected using a progress integration baseline, and then fit to a nontwo state model for 3 transitions.

RESULTS AND DISCUSSION

The development of a TP for IgG with performance that mimics HSP60 begins with identifying a protein affinity reagent that sequesters the target protein IgG at elevated temperatures where protein stability is most vulnerable. Protein binding by NIPAm-based synthetic NPs can be engineered by adjusting the chemical composition of the copolymer, as well as the binding conditions such as temperature, pH, salt, and buffer concentration.[24,39,40] The polymerizable, compositional space to achieve protein binding is vast. Our prior experience narrowed this window to NIPAm copolymer NPs containing hydrophobic and charged functional monomers[31,41−44] and, more specifically for IgG affinity reagents, aliphatic rather than hydrophobic functional groups.[29,30] To this point, NIPAm-based copolymer libraries of 25 NPs were synthesized with aromatic monomers, with and

https://doi.org/10.1021/acs.biomac.4c01492
Biomacromolecules 2025, 26, 2825−2834

without charged monomers, AAc and *N*-(3-Aminopropyl)-methacrylamide (Tables SIA–C). The NPs were synthesized by precipitation polymerization at 65 °C in aqueous solution and purified by dialysis in DI water.[32,44]

The NP library was screened for IgG uptake at 37 °C (Figure S1). IgG binding was found to require both hydrophobic and negatively charged functional monomers. The type of hydrophobic group (branched C4 or linear C4, C6, and C8) impacted IgG uptake to different degrees. The amount of AAc monomer, when used in conjunction with individual hydrophobic groups, was also used to optimize IgG binding. Six promising NIPAm-based hydrogel copolymers were identified from the preliminary screen (Table 1 and Figure 1), resynthesized, and subjected to a more detailed analysis. Their physical properties are summarized in Tables 2 and 3.

Table 3. Summary of Volume Change and LCSTs of NPs[a]

sample name	R_h (nm, DLS)	R_g (nm, MALS)	ΔV ($\times 10^6$ nm^3)	LCST (°C)
tBAm5AAc20	414	248	510	27
tBAm5AAc35	126	81	550	27
OAm5AAc20	83	177	2	27
OAm5AAc35	118	74	4	27
HAm5AAc20	142	104	21	32
HAm5AAc35	139	100	20	DNO

[a]DNO = Did not observe.

Table 4. Pyrene Fluorescence in NP Environment, above and below LCST

sample name	I_1/I_3 (15 °C)	I_1/I_3 (40 °C)
tBAm5AAc35	1.37	1.17
HAm5AAc35	1.05	1.09
OAm5AAc35	0.93	0.94

To provide data to estimate the stoichiometry of IgG–NP complexes, copolymer NPs were analyzed by MALS, RI, and DLS to determine radius of gyration (R_g), hydrodynamic radius (R_h, z-avg), and weight-averaged molecular weight (Mw) (Tables 1–3). The ratio of R_g/R_h was calculated to determine the general topology of the NPs (Table 2). An R_g/R_h ratio of 0.778 suggest the NP exists as a sphere with a uniform internal structure.[32,41,42] NPs with a somewhat denser inner core and a less dense outer shell, a "core–shell" like NP, would have an R_g/R_h ratio less than 0.778.[32,45] Most of the selected NPs had R_g/R_h values of approximately 0.6, which is similar to previously reported lightly cross-linked NiPAm NPs,[45] suggesting these NPs have a slightly denser core. This is the result of a higher cross-linking density in the interior of the NP, a finding attributed to a greater reactivity of the *N*,*N*′-methylenebis(acrylamide) (BIS) monomer used for cross-linking.[46,47] At 2% cross-linking, a lower limit to their average mesh size is estimated to be 15 nm, a size large enough to accommodate proteins such as IgG in the NP interior so the protein-polymer interaction is not limited to the polymer surface, which greatly extends the number of possible interactions between the two.[48,49]

A functioning TP must be readily separated from the protein at RT. NP size and molecular weight are important properties needed to satisfy this requirement. The densities of the NPs were calculated from M_W and size measurements (measured at 25 °C – below LCST, Table 3). The low densities (ρ) of the NPs calculated (0.006–0.009 g/mL) are typical of acrylamide hydrogels below their LCST.[46,47] The NPs were synthesized in the presence of sub CMC concentrations of surfactant to create larger NPs. The NPs ranged in radius from 83–142 nm by DLS, except for **tBAm5AAc20**, which was 414 nm. To evaluate IgG binding by immunoprecipitation, conditions were developed to establish the time, temperature, and RPM (rcf) needed to pelletize suspensions. All NPs were pelleted in as little as 10 min at 15,000 (RPM (21,130 rcf)) at 25 °C.

The LCSTs of each NP were determined by evaluating NP hydrodynamic size by DLS between 10–50 °C, from an approximated inflection point in the thermograms (Table 3). The NPs had LCSTs ranging from 27–32 °C. Prior studies established a general trend that optimal protein binding is found at temperatures greater than LCST.[28,34] NPs in this study bind at temperatures above 32 °C, while losing that capacity below 27 °C; therefore, all screens for NP binding were performed at 37 °C (above the LCST of all NPs tested).

NP Composition and Its Influence on Temperature-Dependent Swelling. The LCST, density, and volume change (swelling ratio) upon passage through the LCST are summarized in Table 3. The swelling ratio is found to be sensitive to the nature of the hydrophobic monomer in the NP. NPs with the most hydrophobic monomers, OAm and HAm, swell much less as they pass through their LCST compared to NPs with less hydrophobic monomers.[50] **OAm5AAc20** and **OAm5AAc35** have a temperature-induced volume change of ~3 × 10^6 nm^3, while NPs with a comparable amount of a slightly less hydrophobic monomer, **HAm5AAc20** and **HAm5AAc35**, have a larger volume change of ~20 × 10^6 nm^3. The NPs with the least hydrophobic monomer, **tBAm5AAc20** and **tBAm5AAc35**, have a dramatic temperature-dependent volume change of ~500 × 10^6 nm^3 (Table 3 and Figure 2). The origin of these trends can be attributed in part to intramolecular NP self-association of the more hydrophobic monomers (HAm and OAm) within each NP. NMR evidence for this is given in Figure S4. Self-association

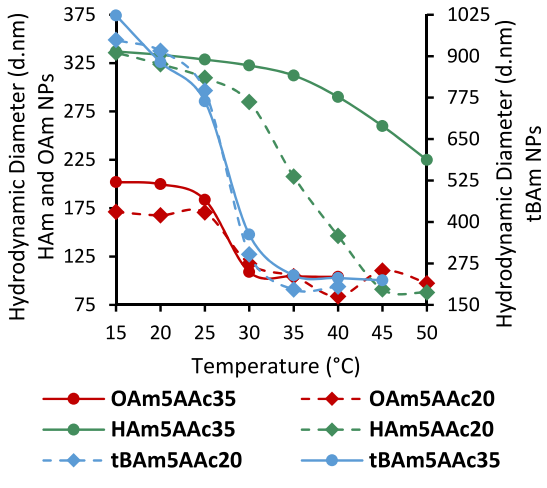

Figure 2. Change in hydrodynamic diameter of different NPs from 15 to 50 °C in DI water (pH 5.5). NPs were incubated at each temperature, starting from 15 °C, for 5 min between each measurement. Temperature was set on the zeta-sizer Nano DLS instrument, and NPs were incubated within the instrument in the cuvette. Note the difference in scale bars for the left- and right-hand axis.

https://doi.org/10.1021/acs.biomac.4c01492
Biomacromolecules 2025, 26, 2825–2834

functions as noncovalent cross-links, reducing the absolute % volume change compared to that observed with the tBAm NPs.[31,51,52] As will be shown, this behavior impacts IgG binding capacity and overall effectiveness as a TP.

Engineering Temperature Control of IgG Capture and Release. With temperature responsiveness data for NPs 1−6, we next turned attention to the temperature effect on IgG capture and release. Since storage and transport of proteins is typically done in buffered solutions, NP−IgG binding was evaluated in SPB (pH 5.5, Figure 3) using centrifugation to

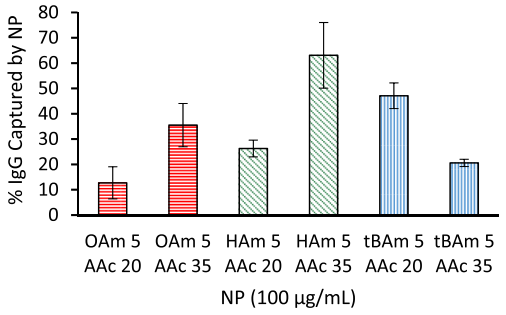

Figure 3. Capture of FITC-IgG (20 μg/mL) using NPs 1−6 in SPB (35 mM, pH 5.5) at 37 °C after 30 min incubation. The NPs were then pelleted via centrifugation, and the supernatant was removed and analyzed using a fluorometer.

pellet the NP protein complex. Changing binding conditions from water to SPB (35 mM, pH 5.5) did not significantly affect the NP−IgG binding trends (Figures 3 and S1).

To evaluate the temperature-induced release, the pelleted NP−IgG complexes (Figure 3) produced by centrifugation from IgG-NP solutions in SPB (35 mM, pH 5.5) at 37 °C were reconstituted in PBS (35 mM, pH 7.3, 150 mM NaCl) and cooled to 25 °C, a temperature below the measured LCST (27−32 °C), for 30 min. The NPs then were pelleted again, and the supernatant was analyzed for the presence of FITC-IgG (Figure 4). Although the capacity of individual NP's differed (Figure 3), all NPs showed efficient release of bound IgG (Figure 4).

Hydrophobicity of NPs above and below LCST. HSP60 functions by binding a partially denatured protein in

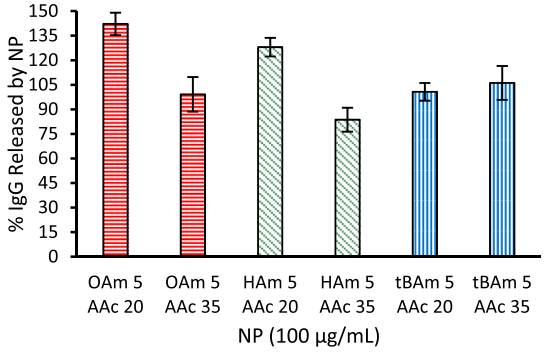

Figure 4. Percent release of IgG from the NP−IgG complex (Figure 3) in PBS (35 mM, pH 7.3, 150 mM NaCl) solution at 25 °C after 30 min incubation. Note, the IgG capacity of each NP differs, but the above calculations were based on previously calculated captured IgG amounts, and not the original amount of IgG used. Percentages greater than 100 arise from the cumulative errors of both experiments, which are not represented in this Figure.

a hydrophobic binding pocket. Protein refolding takes place following an ATP-driven conformational change that transforms the microenvironment from hydrophobic to hydrophilic,[53] providing an opportunity for the protein to refold in a hydrophilic environment. NIPAm polymers below their LCST are more hydrophilic and water swollen than when above their LCST.[54] However, the introduction of both hydrophobic and charged comonomers may complicate this analysis. To establish if the NPs in this study parallel this behavior, a fluorescent probe, pyrene, was used to estimate the temperature-dependent hydrophobicity change in three representative candidates (**OAm5AAc35**, **HAm5AAc35**, and **tBAm5AAc35**) as the NP passes through its LCST (Figure 5). The ratio

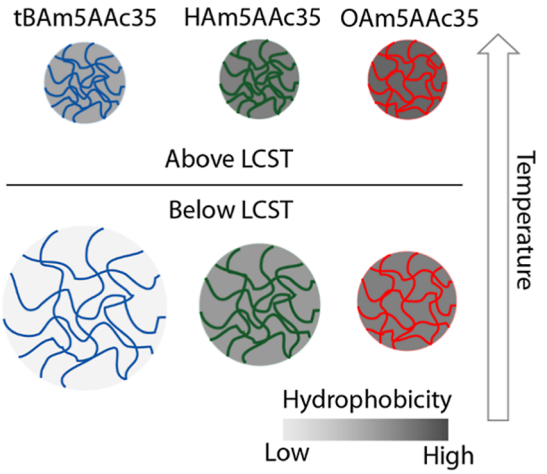

Figure 5. Size and hydrophobicity of NPs above and below LCST as measured by a pyrene fluorescence probe. The data is summarized in Table 4.

between the intensities of the first and third peaks (I_1/I_3, 375 and 386 nm) in the fluorescence spectrum of pyrene is sensitive to the polarity of the local environment. The I_1/I_3 value decreases with increasing hydrophobicity.[55]

The data shows the I_1/I_3 values decrease with increasing hydrophobicity of the side chains (**OAm5AAc35** < **HAm5AAc35** < **tBAm5AAc35**). **OAm5AAc35** exhibited no change in polarity upon passing through the LCST, while **HAm5AAc35** was shown to be slightly more hydrophobic above the LCST than below. **tBAm5AAc35**, on the other hand, was significantly more hydrophobic above its LCST than below. Native and metastable IgG binds to the hydrophobic **tBAm5AAc35** (I_1/I_3 = 1.17) above its LCST. Upon cooling below its LCST, **tBAm5AAc35** becomes more hydrophilic (I_1/I_3 = 1.37), ultimately releasing the bound IgG. In contrast, there was little or no change in microenvironment hydrophilicity as the temperature was lowered for **HAm5AAc35** and **OAm5AAc35**, an observation that might be explained by the intramolecular aggregation (noncovalent cross-links) of the HAm and OAm side chains.[31,51,52] We note a caveat with the interpretation of these experiments; both **HAm5AAc35** and **OAm5AAc35** NPs undergo some swelling and release their IgG cargo, measuring the average NP hydrophilicity or hydrophobicity is complicated in these inhomogeneous materials by the possible preferential localization of the pyrene probe in hydrophobic domains of **HAm5AAc35** and **OAm5AAc35.** Nevertheless, on the basis of swelling ratio

https://doi.org/10.1021/acs.biomac.4c01492
Biomacromolecules 2025, 26, 2825−2834

and polarity change, **tBAm5AAc35** becomes the most promising candidate.

Determining Structural Integrity of Bound-Released IgG Using Circular Dichroism and SEC-HPLC. The temperature-dependent catch and release of IgG is valuable if the released protein retains its structural integrity. The effectiveness of the abiotic TPs in stabilizing and releasing IgG following exposure to thermal stress (60 °C, 5 min) was first evaluated by SEC (Figure 6). A standard set of conditions

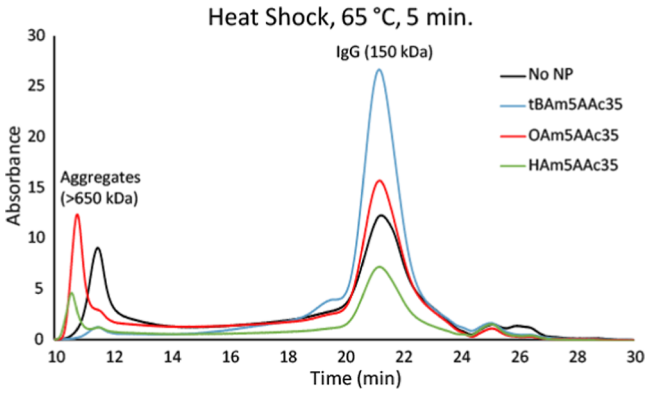

Figure 6. SEC-HPLC analysis of IgG solutions in the presence and absence of NPs after thermal stress.

was used to allow comparison of the candidate TPs. Solutions of IgG with and without NP TPs were heated for 5 min at 60 °C, pelleted (60 °C) via centrifugation, and the supernatant with any potentially unbound IgG was removed. The pellet was then reconstituted in PBS, incubated at 4 °C for 2 h, pelleted via centrifugation, and the supernatant containing recovered protein was removed and analyzed by SEC-HPLC. The peak at ∼21 min is identified as native IgG. The peak at ∼11 min is assigned to IgG aggregates.[56,57] From this data (Figure 6), we observe that the IgG solution in the absence of TPs, when heated for 5 min at 60 °C without NPs, shows a large peak at ∼11 min, as well as a smaller native IgG peak at ∼21 min, implying a significant portion of NP bound IgG aggregated during heating. The supernatant from the **OAm5AAc35** and **HAm5AAc35** solutions, NPs that showed higher capacity for IgG (Figure 3), also showed two peaks on SEC-HPLC (Figure 6) at ∼11 and at ∼21 min, indicating that although some native IgG is recovered, large quantities of IgG aggregates are also formed. In contrast, the supernatant from the **tBAm5AAc35** solution showed a single peak on SEC-HPLC at ∼21 min, establishing that **tBAm5AAc35** is most effective in preventing IgG aggregation. Although not a stringent criteria, on the basis of the SEC-HPLC retention time, the recovered IgG retained its native state.

Next, those same supernatant solutions with recovered IgG were analyzed via circular dichroism spectroscopy (CD, Figures 7 and S3) to determine if the recovered IgG (the peak that was associated with native IgG seen on SEC-HPLC at ∼21 min) had retained its native structure following exposure to thermal stress.[57] From the data (Figure 7), the ellipticity of IgG recovered in the supernatant from the thermal protocol was superimposable with that of native IgG, revealing that the IgG recovered from all solutions had retained its native secondary structure. These criteria, coupled with a DSC study of NP−IgG complexes (vide infra), establish that IgG retains its native structure following thermal stress. Although the

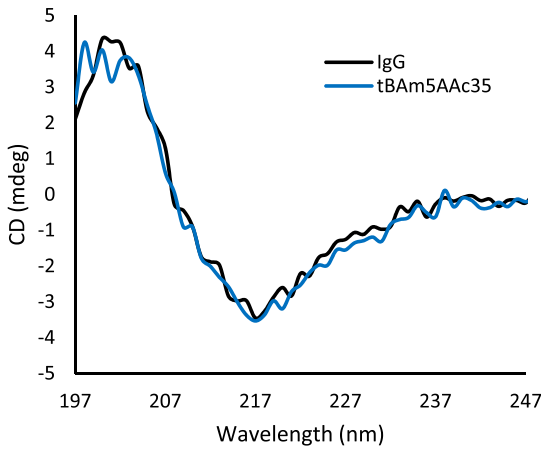

Figure 7. CD analysis of recovered IgG after thermal stress. A control sample shows the CD spectrum of native IgG without heating (IgG) was compared to a sample are IgG heated to 60 °C for 5 min with **tBAm5AAc35**. The NP/IgG solution was first pelleted (SPB, pH 5.5), and unbound IgG was removed. The NP−IgG complex was then reconstituted in PBS to encourage release of IgG into solution, the NPs were pelleted again, and the supernatant containing released IgG was analyzed.

results are consistent with but do not prove IgG function is retained. For the study, we chose polyclonal IgG rather than a specific functional antibody. Polyclonal IgG was selected for this study because it encompasses proteins with a wide range of isoelectric points (pI) that encompass most therapeutically important antibodies. Our rationale was that developing conditions to protect this diverse protein mixture, rather than focusing on a specific antibody, would yield a more general and versatile approach for sequestering, protecting, and releasing a broad spectrum of therapeutic IgGs, offering greater value compared to targeting a single antibody.

Estimates of NP−IgG Stoichiometry. The results identify significant differences in NP effectiveness in preserving native structure and preventing aggregation. There are a number of chemical and physical differences between the three NPs. For example, possible contributing factors in performance could arise from differences in NP hydrophobicity. Greater amounts of IgG aggregation were found in the presence of the more hydrophobic OAm and HAm NPs, resulting in greater amounts of IgG aggregation. Hydrophobic polymers have been reported in some cases to bring about the denaturation of proteins;[58,59] however, the results from the simple pyrene hydrophobic probe reveal that these complex hydrogel copolymers are not readily cataloged as hydrophobic or hydrophilic. This does not, however, eliminate contributions from NPs containing more hydrophobic monomers. To pursue other lines of reasoning, we considered NP−IgG stoichiometry. On a per weight basis, **OAm5AAc35** and **HAm5AAc5** NPs bind more IgG compared to **tBAm5AAc35**. The less hydrophobic **tBAm5AAc35** NP sequesters and releases IgG with little to no aggregation. Recalling that HSP60 binds and isolates metastable proteins, we considered if the number of IgG molecules per NP relates to the performance of these NPs as a TP. To estimate the concentration of bound protein per unit volume of the NP, we assume that IgG binds throughout the NP. Although there is some information to support this assumption,[60,61] as well as estimates of polymer mesh size (at 2% cross-linking) large enough to accommodate IgG, there is insufficient data at present to generalize this observation.

https://doi.org/10.1021/acs.biomac.4c01492
Biomacromolecules 2025, 26, 2825−2834

Despite this caveat, we evaluated NP−IgG stoichiometry from available size, molecular weight, and density information acquired by a combination of DLS and SEC-HPLC data. The results are summarized in Table 5.

Table 5. Molar Ratio of Bound IgG per NP[a]

sample name	MW (MALS)	IgG/NP
tBAm5AAc35	5.6×10^6	77
HAm5AAc35	5.9×10^7	2485
OAm5AAc35	3.1×10^7	743

[a]NP molarity was calculated from the NP MW (MALS), and the number of moles of IgG bound by each NP at 40 °C. Data used for the calculation is found in the Supporting Information.

The most effective TP (**tBAm5AAc35**) had 10−30 times lower IgG loading compared to **OAm5AAc35** and **HAm5AAc35**. We conclude that the IgG concentration within the NP is an important contributing factor to its functioning as a TP.

VP-DSC Analysis of T_m of IgG. Previous sections provided evidence that TPs with slightly varying compositions differ significantly in their effectiveness at preventing thermal denaturation and aggregation of IgG. While these two processes are kinetically independent, they are closely related. Thermograms of IgG show multiple endothermic transitions arising from distinct denaturation steps. Aggregation, on the other hand, depends on concentrations of aggregation-prone conformational states of IgG and can be either exo- or endothermic, depending on the conditions.[59,60,62,63] Despite the complexity of these systems, we hoped to learn more about the differences of NP performance by analyzing the thermal behavior of NP−IgG complexes when heated beyond IgG's melting temperature (T_m) of approximately 60 °C. The broad thermogram of IgG alone (Figure 8, black) ranged from 25 to 70 °C with a maximum of ∼45 °C (T_m), which reflects the unfolding of multiple IgG domains as well as the polyclonal nature of the IgG used.[64,65] Upon adding either **HAm5AAc35** or **OAm5AAc35** to IgG, the endothermic peaks in the thermograms were significantly reduced, and the T_m shifted from 45 to 57 °C and 70 °C, respectively (Table S3). In contrast, when **tBAm5AAc35** was added to IgG, the endothermic peak disappeared entirely. The magnitude of the endothermic peak is affected by the number of hydrophobic side chains that are exposed due to solvation changes around the hydrophobic side chains during the unfolding process.[66] The reduction in the endotherm with NP−IgG complexes may be due to a reduction in the availability of the exposed hydrophobic side chains of unfolded IgG due to binding to the NP TP. This result, along with the IgG recovery data, highlights the remarkable effect of **tBAm5AAc35** in stabilizing IgG and preventing both denaturation and aggregation under thermal stress, up to 90 °C (∼30 °C above IgG's T_m)! In contrast, **OAm5AAc35** and **HAm5AAc35** only partially prevented IgG aggregation. The three NPs differ in chemical composition, but as discussed earlier, there are likely multiple factors that account for these differences. By analogy to HSP60, a key function of chaperones is to separate or dilute aggregation-prone proteins and provide conditions conducive to refolding prior to their release. The IgG capacity of these NPs is relatively low, which must contribute to their performance. Our findings highlight that **tBAm5AAc35** exhibits a unique combination of properties, notably its ability to reduce the effective concentration of stressed proteins and create an environment that promotes refolding upon cooling.

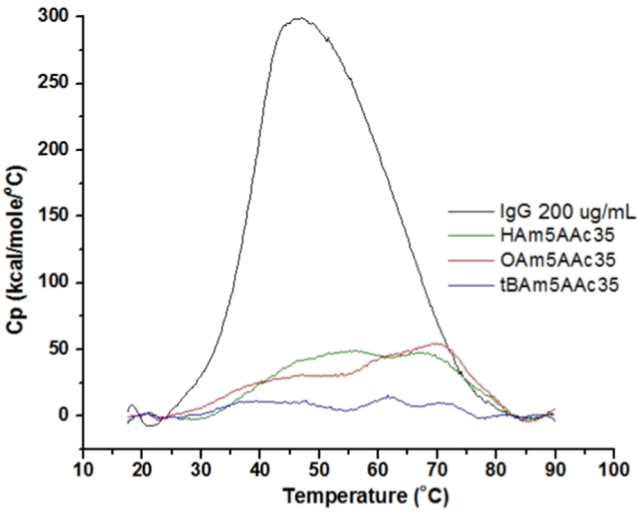

Figure 8. VP-DSC trace of IgG (200 μg/mL) with the addition of various NPs (1 mg/mL). Solutions were heated from 15−90 °C at 50 °C/h under ∼25 psi. Same conditions were used for all samples, regardless of NP capacity differences.

CONCLUSIONS

Heating IgG above physiological temperatures that approach or exceed T_m (∼60 °C), even for brief periods of time, can result in substantial irreversible aggregation. In this report, we describe a synthetic hydrogel copolymer NP, a TP that serves as a functional equivalent of HSP60, a biological chaperone protein responsible for correcting metastable or misfolded proteins prior to their aggregation. To achieve this biological mimicry, we screened a small library of hydrogel NPs that bind IgG ($K_d \sim 10^{-6}$). Attributes associated with HSP60 were selected from the candidates. NP function derives in part from its autonomous affinity for IgG above 27 °C, which is well under the temperature at which IgG begins to unfold and denature (T_m). NP−IgG binding arises from the collapsed, partially desolvated hydrophobic nature of the NP at temperatures above 27 °C and the hydrophobic domains of the native and partially denatured protein. When native IgG is subjected to a thermal cycle that involves heating to 60 °C for 5 min followed by cooling back to RT substantial irreversible aggregation is observed. In the presence of candidate NPs that span a range of chemical composition, the degree of irreversible aggregation of NP bound IgG varied from almost no effect to complete suppression of aggregation. Upon cooling below their LCST, the NP−IgG complex dissociates. Using I_1/I_3 values from pyrene fluorescence experiments as an index of hydrophobicity, thermal analysis, IgG uptake studies, and NP molecular weight information, trends in IgG capacity and suppression of aggregation were revealed.

At elevated temperatures, the partially desolvated, collapsed NP is more hydrophobic and has affinity for native and partially unfolded IgG. Upon cooling, the NPs swell and are transformed to a more hydrated hydrophilic microenvironment. The bound, partially denatured IgG is then transferred to a more hydrophilic microenvironment, releasing the protein. This transition takes place rapidly as temperature drops, providing sufficient time for IgG to refold if needed. The most

https://doi.org/10.1021/acs.biomac.4c01492
Biomacromolecules 2025, 26, 2825−2834

effective TP (**tBAm5AAc35**) had 10−30 times lower IgG loading compared to **OAm5AAc35** and **HAm5AAc35**. We conclude that the IgG concentration within the NP is an important contributing factor to its functioning as a TP. These materials offer the potential to serve as an autonomous protectant for IgG in areas that lack suitable cold chain and provide therapies that would not otherwise be readily available.

■ ASSOCIATED CONTENT

Supporting Information

The Supporting Information is available free of charge at https://pubs.acs.org/doi/10.1021/acs.biomac.4c01492.

NP molarity calculation; compositions and sizes of copolymer NPs; density and LCSTs of NPs; titration data for AAc content; percentage of FITC-IgG remaining in solution after addition of NPs at 37 °C; pyrene fluorescence results; CD traces of recovered IgG after thermal stress; and denaturation temperatures and enthalpy of thermal denaturation by VP-DSC (PDF)

■ AUTHOR INFORMATION

Corresponding Author

Kenneth J. Shea − *Department of Chemistry, University of California, Irvine, Irvine, California 92697, United States;* orcid.org/0000-0001-5926-0059; Email: kjshea@uci.edu

Authors

Beverly Chou − *Department of Chemistry, University of California, Irvine, Irvine, California 92697, United States*

Rishad J. Dalal − *Department of Chemistry, University of California, Irvine, Irvine, California 92697, United States*

Complete contact information is available at: https://pubs.acs.org/10.1021/acs.biomac.4c01492

Author Contributions

B.C. and K.J.S. designed the research and experiments. B.C. and R.D. performed the experiments. B.C. and K.J.S. discussed the results, commented on the paper, and wrote the manuscript. All authors have given their approval to the final version of the manuscript.

Notes

The authors declare no competing financial interest.

■ ACKNOWLEDGMENTS

The work was supported by the US National Science Foundation (Grant No. DMR 1308363).

■ REFERENCES

(1) Walsh, G. Biopharmaceutical benchmarks 2018. *Nat. Biotechnol.* **2018**, *36* (12), 1136−1145.

(2) Biologics Market Size. Report on Industry Size & Market Share Analysis - Growth Trends & Forecasts (2024−2029). https://www.mordorintelligence.com/industry-reports/biologics-market (accessed July 26, 2024).

(3) Castelli, M. S.; McGonigle, P.; Hornby, P. J. The pharmacology and therapeutic applications of monoclonal antibodies. *Pharmacol. Res. Perspect.* **2019**, *7* (6), No. e00535.

(4) Kumar, V.; Barwal, A.; Sharma, N.; Mir, D. S.; Kumar, P.; Kumar, V. Therapeutic proteins: developments, progress, challenges, and future perspectives. *3 Biotech* **2024**, *14* (4), 112.

(5) Akbarian, M.; Chen, S. H. Instability Challenges and Stabilization Strategies of Pharmaceutical Proteins. *Pharmaceutics* **2022**, *14* (11), 2533.

(6) Technical report # 39: cold chain guidance for medicinal products: maintaining the quality of temperature-sensitive medicinal products through the transportation environment. Parenteral Drug Association. *PDA J. Pharm. Sci. Technol.* **2005**, *59* (3 Suppl TR39), 1−12.

(7) Yu, Y. B.; Briggs, K. T.; Taraban, M. B.; Brinson, R. G.; Marino, J. P. Grand Challenges in Pharmaceutical Research Series: Ridding the Cold Chain for Biologics. *Pharm. Res.* **2021**, *38* (1), 3−7.

(8) Mehta, R.; Singhal, P.; Singh, H.; Damle, D.; Sharma, A. K. Insight into thermophiles and their wide-spectrum applications. *3 Biotech* **2016**, *6* (1), 81.

(9) *Temperature-sensitive Health Products in the Expanded Programme on Immunization Cold Chain*. WHO/UNICEF, 2020.

(10) Dinerstein, C. Snake venom Snake Bites, Camels and Cold-Chain Logistics. 2021. https://www.acsh.org/news/2021/11/26/snake-bites-camels-and-cold-chain-logistics-15951 (accessed July 26, 2024).

(11) Hu, C.; Yang, J.; Qi, Z.; Wu, H.; Wang, B.; Zou, F.; Mei, H.; Liu, J.; Wang, W.; Liu, Q. Heat shock proteins: Biological functions, pathological roles, and therapeutic opportunities. *MedComm* **2022**, *3* (3), No. e161.

(12) Kim, Y. E.; Hipp, M. S.; Bracher, A.; Hayer-Hartl, M.; Ulrich Hartl, F. Molecular chaperone functions in protein folding and proteostasis. *Annu. Rev. Biochem.* **2013**, *82*, 323−355.

(13) Krishnan-Sivadoss, I.; Mijares-Rojas, I. A.; Villarreal-Leal, R. A.; Torre-Amione, G.; Knowlton, A. A.; Guerrero-Beltran, C. E. Heat shock protein 60 and cardiovascular diseases: An intricate love-hate story. *Med. Res. Rev.* **2021**, *41* (1), 29−71.

(14) Kaushik, J. K.; Bhat, R. Why is trehalose an exceptional protein stabilizer? An analysis of the thermal stability of proteins in the presence of the compatible osmolyte trehalose. *J. Biol. Chem.* **2003**, *278* (29), 26458−26465.

(15) Olsson, C.; Jansson, H.; Swenson, J. The Role of Trehalose for the Stabilization of Proteins. *J. Phys. Chem. B* **2016**, *120* (20), 4723−4731.

(16) Liu, B.; Zhou, X. Freeze-drying of proteins. *Methods Mol. Biol.* **2015**, *1257*, 459−476.

(17) Sivasankaran, R. P.; Snell, K.; Kunkel, G.; Georgiou, P. G.; Puente, E. G.; Maynard, H. D. Polymer-mediated protein/peptide therapeutic stabilization: Current progress and future directions. *Prog. Polym. Sci.* **2024**, *156*, 101867.

(18) De, M.; Rotello, V. M. Synthetic "chaperones": nanoparticle-mediated refolding of thermally denatured proteins. *Chem. Commun. (Camb)* **2008**, *30*, 3504−3506.

(19) Takahashi, H.; Sawada, S.; Akiyoshi, K. Amphiphilic polysaccharide nanoballs: a new building block for nanogel biomedical engineering and artificial chaperones. *ACS Nano* **2011**, *5* (1), 337−345.

(20) Liu, X.; Liu, Y.; Zhang, Z.; Huang, F.; Tao, Q.; Ma, R.; An, Y.; Shi, L. Temperature-responsive mixed-shell polymeric micelles for the refolding of thermally denatured proteins. *Chemistry* **2013**, *19* (23), 7437−7442.

(21) Ma, F. H.; Li, C.; Liu, Y.; Shi, L. Mimicking Molecular Chaperones to Regulate Protein Folding. *Adv. Mater.* **2020**, *32* (3), No. e1805945.

(22) Hanpanich, O.; Maruyama, A. Artificial chaperones: From materials designs to applications. *Biomaterials* **2020**, *254*, 120150.

(23) Balchin, D.; Hayer-Hartl, M.; Hartl, F. U. In vivo aspects of protein folding and quality control. *Science* **2016**, *353* (6294), aac4354.

(24) O'Brien, J.; Shea, K. J. Tuning the Protein Corona of Hydrogel Nanoparticles: The Synthesis of Abiotic Protein and Peptide Affinity Reagents. *Acc. Chem. Res.* **2016**, *49* (6), 1200−1210.

(25) Beierle, J. M.; Yoshimatsu, K.; Chou, B.; Mathews, M. A. A.; Lesel, B. K.; Shea, K. J. Polymer Nanoparticle Hydrogels with

Autonomous Affinity Switching for the Protection of Proteins from Thermal Stress. *Angew. Chem., Int. Ed.* **2014**, *53* (35), 9275−9279.
(26) Keller, S.; Toebes, B. J.; Wilson, D. A. Active, Autonomous, and Adaptive Polymeric Particles for Biomedical Applications. *Biomacromolecules* **2019**, *20* (3), 1135−1145.
(27) Nakamoto, M.; Nonaka, T.; Shea, K. J.; Miura, Y.; Hoshino, Y. Design of Synthetic Polymer Nanoparticles That Facilitate Resolubilization and Refolding of Aggregated Positively Charged Lysozyme. *J. Am. Chem. Soc.* **2016**, *138*, 4282−4285.
(28) Yoshimatsu, K.; Lesel, B. K.; Yonamine, Y.; Beierle, J. M.; Hoshino, Y.; Shea, K. J. Temperature-Responsive "Catch and Release" of Proteins by using Multifunctional Polymer-Based Nanoparticles. *Angew. Chem., Int. Ed.* **2012**, *51* (10), 2405−2408.
(29) Onogi, S.; Lee, S. H.; Fruehauf, K. R.; Shea, K. J. Abiotic Stimuli-Responsive Protein Affinity Reagent for IgG. *Biomacromolecules* **2021**, *22*, 2641−2648.
(30) Hoshino, Y.; Arata, Y.; Yonamine, Y.; Lee, S.-H.; Yamasaki, A.; Tsuhara, R.; Yano, K.; Shea, K. J.; Miura, Y. Preparation of nanogel-immobilized porous gel beads for affinity separation of proteins: fusion of nano and micro gel materials. *Polym. J.* **2015**, *47*, 220−225.
(31) Chou, B.; Mirau, P.; Jiang, T.; Wang, S. W.; Shea, K. J. Tuning Hydrophobicity in Abiotic Affinity Reagents: Polymer Hydrogel Affinity Reagents for Molecules with Lipid-like Domains. *Biomacromolecules* **2016**, *17* (5), 1860−1868.
(32) Yoshimatsu, K.; Koide, H.; Hoshino, Y.; Shea, K. J. Preparation of abiotic polymer nanoparticles for sequestration and neutralization of a target peptide toxin. *Nat. Protoc.* **2015**, *10* (4), 595−604.
(33) Hoshino, Y.; Urakami, T.; Kodama, T.; Koide, H.; Oku, N.; Okahata, Y.; Shea, K. J. Design of Synthetic Polymer Nanoparticles that Capture and Neutralize a Toxic Peptide. *Small* **2009**, *5* (13), 1562−1568.
(34) Hoshino, Y.; Haberaecker, W. W.; Kodama, T.; Zeng, Z. Y.; Okahata, Y.; Shea, K. J. Affinity Purification of Multifunctional Polymer Nanoparticles. *J. Am. Chem. Soc.* **2010**, *132* (39), 13648−13650.
(35) Zeng, Z. Y.; Hoshino, Y.; Rodriguez, A.; Yoo, H. S.; Shea, K. J. Synthetic Polymer Nanoparticles with Antibody-like Affinity for a Hydrophilic Peptide. *ACS Nano* **2010**, *4* (1), 199−204.
(36) Hoshino, Y.; Koide, H.; Oyama, D.; Yonamine, Y.; Lee, S. H.; Oku, N.; Shea, K. J. *Design of polymer nanoparticles that are capable of neutralizing toxicity of fetal proteins*, 2011.
(37) Hoshino, Y.; Koide, H.; Furuya, K.; Haberaecker, W. W.; Lee, S. H.; Kodama, T.; Kanazawa, H.; Oku, N.; Shea, K. J. The rational design of a synthetic polymer nanoparticle that neutralizes a toxic peptide in vivo. *P Natl. Acad. Sci. USA* **2012**, *109* (1), 33−38.
(38) Mcphee, W.; Tam, K. C.; Pelton, R. Poly(N-Isopropylacrylamide) Latices Prepared with Sodium Dodecyl-Sulfate. *J. Colloid Interface Sci.* **1993**, *156* (1), 24−30.
(39) Liu, M.; Huang, R.; Weisman, A.; Yu, X.; Lee, S. H.; Chen, Y.; Huang, C.; Hu, S.; Chen, X.; Tan, W.; Liu, F.; Chen, H.; Shea, K. J. Synthetic Polymer Affinity Ligand for Bacillus thuringiensis (Bt) Cry1Ab/Ac Protein: The Use of Biomimicry Based on the Bt Protein-Insect Receptor Binding Mechanism. *J. Am. Chem. Soc.* **2018**, *140* (22), 6853−6864.
(40) Honda, R.; Gyobu, T.; Shimahara, H.; Miura, Y.; Hoshino, Y. Electrostatic Interactions between Acid-/Base-Containing Polymer Nanoparticles and Proteins: Impact of Polymerization pH. *ACS Appl. Bio Mater.* **2020**, *3* (6), 3827−3834.
(41) Arleth, L.; Xia, X. H.; Hjelm, R. P.; Wu, J. Z.; Hu, Z. B. Volume transition and internal structures of small poly(N-isopropylacrylamide) microgels. *J. Polym. Sci. Pol Phys.* **2005**, *43* (7), 849−860.
(42) Brewer, A. K.; Striegel, A. M. Characterizing the size, shape, and compactness of a polydisperse prolate ellipsoidal particle via quadruple-detector hydrodynamic chromatography. *Analyst* **2011**, *136* (3), 515−519.
(43) O'Brien, J.; Lee, S. H.; Onogi, S.; Shea, K. J. Engineering the Protein Corona of a Synthetic Polymer Nanoparticle for Broad-Spectrum Sequestration and Neutralization of Venomous Biomacromolecules. *J. Am. Chem. Soc.* **2016**, *138* (51), 16604−16607.
(44) Weisman, A.; Chen, Y. A.; Hoshino, Y.; Zhang, H.; Shea, K. Engineering nanoparticle antitoxins utilizing aromatic interactions. *Biomacromolecules* **2014**, *15* (9), 3290−3295.
(45) Tande, B. M.; Wagner, N. J.; Mackay, M. E.; Hawker, C. J.; Jeong, M. Viscosimetric, hydrodynamic, and conformational properties of dendrimers and dendrons. *Macromolecules* **2001**, *34* (24), 8580−8585.
(46) Fernandez-Barbero, A.; Fernandez-Nieves, A.; Grillo, I.; Lopez-Cabarcos, E. Structural modifications in the swelling of inhomogeneous microgels by light and neutron scattering. *Phys. Rev. E:Stat., Nonlinear, Soft Matter Phys.* **2002**, *66* (5), 051803.
(47) Smith, M. H.; Lyon, L. A. Tunable Encapsulation of Proteins within Charged Microgels. *Macromolecules* **2011**, *44* (20), 8154−8160.
(48) Canal, T.; Peppas, N. A. Correlation between mesh size and equilibrium degree of swelling of polymeric networks. *J. Biomed. Mater. Res.* **1989**, *23* (10), 1183−1193.
(49) Chai, Q.; Jiao, Y.; Yu, X. Hydrogels for Biomedical Applications: Their Characteristics and the Mechanisms behind Them. *Gels* **2017**, *3* (1), 6.
(50) Foster, J. C.; Akar, I.; Grocott, M. C.; Pearce, A. K.; Mathers, R. T.; O'Reilly, R. K. 100th Anniversary of Macromolecular Science Viewpoint: The Role of Hydrophobicity in Polymer Phenomena. *ACS Macro Lett.* **2020**, *9* (11), 1700−1707.
(51) Pekar, M. Hydrogels with micellar hydrophobic (nano)-domains. *Front. Mater.* **2015**, *1*, 35.
(52) Wu, J.; Li, H.; Zhang, N.; Zheng, Q. Micelle-Containing Hydrogels and Their Applications in Biomedical Research. *Gels* **2024**, *10* (7), 471.
(53) Ranford, J. C.; Coates, A. R.; Henderson, B. Chaperonins are cell-signalling proteins: the unfolding biology of molecular chaperones. *Expert Rev. Mol. Med.* **2000**, *2* (8), 1−17.
(54) Cabaleiro-Lago, C.; Quinlan-Pluck, F.; Lynch, I.; Lindman, S.; Minogue, A. M.; Thulin, E.; Walsh, D. M.; Dawson, K. A.; Linse, S. Inhibition of Amyloid beta Protein Fibrillation by Polymeric Nanoparticles. *J. Am. Chem. Soc.* **2008**, *130* (46), 15437−15443.
(55) Dong, D. C.; Winnik, M. A. The Py scale of solvent polarities. Solvent effects on the vibronic fine structure of pyrene fluorescence and empirical correlations with E_T and Y values. *Photochem. Photobiol.* **1982**, *35*, 17−21.
(56) Senga, Y.; Honda, S. Suppression of Aggregation of Therapeutic Monoclonal Antibodies during Storage by Removal of Aggregation Precursors Using a Specific Adsorbent of Non-Native IgG Conformers. *Bioconjug Chem.* **2018**, *29* (10), 3250−3261.
(57) Joshi, V.; Shivach, T.; Yadav, N.; Rathore, A. S. Circular Dichroism Spectroscopy as a Tool for Monitoring Aggregation in Monoclonal Antibody Therapeutics. *Anal. Chem.* **2014**, *86* (23), 11606−11613.
(58) Gray, J. J. The interaction of proteins with solid surfaces. *Curr. Opin. Struct. Biol.* **2004**, *14* (1), 110−115.
(59) Satzer, P.; Svec, F.; Sekot, G.; Jungbauer, A. Protein adsorption onto nanoparticles induces conformational changes: Particle size dependency, kinetics, and mechanisms. *Eng. Life Sci.* **2016**, *16* (3), 238−246.
(60) Cho, K.; Fasoli, J. B.; Yoshimatsu, K.; Shea, K. J.; Corn, R. M. Measuring melittin uptake into hydrogel nanoparticles with near-infrared single nanoparticle surface plasmon resonance microscopy. *Anal. Chem.* **2015**, *87* (9), 4973−4979.
(61) Fruehauf, K. R.; Kim, T. I.; Nelson, E. L.; Patterson, J. P.; Wang, S. W.; Shea, K. J. Metabolite Responsive Nanoparticle-Protein Complex. *Biomacromolecules* **2019**, *20* (7), 2703−2712.
(62) Vermeer, A. W. P.; Norde, W. The thermal stability of immunoglobulin: Unfolding and aggregation of a multi-domain protein. *Biophys. J.* **2000**, *78* (1), 394−404.
(63) Nemergut, M.; Zoldak, G.; Schaefer, J. V.; Kast, F.; Miskovsky, P.; Pluckthun, A.; Sedlak, E. Analysis of IgG kinetic stability by differential scanning calorimetry, probe fluorescence and light scattering. *Protein Sci.* **2017**, *26*, 2229−2239.

https://doi.org/10.1021/acs.biomac.4c01492
Biomacromolecules 2025, 26, 2825−2834

(64) Martin, N.; Ma, D. W.; Herbet, A.; Boquet, D.; Winnik, F. M.; Tribet, C. Prevention of Thermally Induced Aggregation of IgG Antibodies by Noncovalent Interaction with Poly(acrylate) Derivatives. *Biomacromolecules* **2014**, *15* (8), 2952−2962.
(65) Vermeer, A. W. P.; Norde, W.; van Amerongen, A. The unfolding/denaturation of immunogammaglobulin of isotype 2b and its F-ab and F-c fragments. *Biophys. J.* **2000**, *79* (4), 2150−2154.
(66) Quinn, C. F. D. N. A. *Determining Thermal Stability of Antibodies with a Nano DSC*; TA Instruments, 2011.

https://doi.org/10.1021/acs.biomac.4c01492
Biomacromolecules 2025, 26, 2825−2834